European Journal of Medicinal Chemistry 44 (2009) 1554–1569

Contents lists available at ScienceDirect

European Journal of Medicinal Chemistry

journal homepage: http://www.elsevier.com/locate/ejmech

Original article

The porphyrin–fullerene nanoparticles to promote the ATP overproduction in myocardium: $^{25}Mg^{2+}$-magnetic isotope effect

S.M. Rezayat [a], S.V.S. Boushehri [a], B. Salmanian [a], A.H. Omidvari [a], S. Tarighat [a], S. Esmaeili [a], S. Sarkar [b], N. Amirshahi [c,*], R.N. Alyautdin [c], M.A. Orlova [d], I.V. Trushkov [d], A.L. Buchachenko [e], K.C. Liu [e], D.A. Kuznetsov [e]

[a] School of Medicine, Tehran University of Medical Sciences, Tehran, Iran
[b] Research Center for Science and Technology in Medicine, TUMS, Tehran, Iran
[c] School of Pharmacy, I.M. Sechenov Moscow Medical Academy, Moscow, Russia
[d] Department of Chemistry, M.V. Lomonosov Moscow State University, Moscow, Russia
[e] N.N. Semenov Institute for Chemical Physics, Russian Academy of Sciences, Moscow, Russia

ARTICLE INFO

Article history:
Received 25 February 2008
Received in revised form 17 July 2008
Accepted 17 July 2008
Available online 31 July 2008

Keywords:
Porphyrin–fullerenes
Myocardium hypoxia
$^{25}Mg^{2+}$-magnetic isotope effect
ATP overproduction

ABSTRACT

This is a first case ever reported on the fullerene-based low toxic *nanocationite particles* (porphyrin adducts of cyclohexyl fullerene-C_{60}) designed for targeted delivery of the paramagnetic magnesium stable isotope to the heart muscle providing a sharp clinical effect close to about 80% recovery of the tissue hypoxia symptoms in less than 24 h after a single injection (0.03–0.1 LD_{50}). A whole principle of this therapy is novel: $^{25}Mg^{2+}$-magnetic isotope effect selectively stimulates the ATP overproduction in the oxygen-depleted cells due to $^{25}Mg^{2+}$ released by the nanoparticles. Being membranotropic cationites, these "smart nanoparticles" release the overactivating paramagnetic cations *only* in response to the metabolic acidic shift. The resulting positive changes in the heart cell energy metabolism may help to prevent and/or treat the local myocardial hypoxic disorders and, hence, protect the heart muscle from a serious damage in a vast variety of the hypoxia-caused clinical situations including both doxorubicin and 1-methylnicotineamide cardiotoxic side effects. Both pharmacokinetics and pharmacodynamics of the drug proposed make it suitable for safe and efficient administration in either single or multi-injection (acute or chronic) therapeutic schemes.

1. Introduction

A development of pharmacologically appropriate, i.e. safe and efficient, nanocarriers for Mg^{2+} ions has been initiated by the recent discovery of a so-called magnesium-25 magnetic isotope effect in biophysical control over the energy supplying processes in mitochondria. Thus, the only magnetic isotope of magnesium, ^{25}Mg, is proven to be a specific over-activator for most Mg^{2+}-dependent reactions of ATP production taking place in a cell. Noteworthy, this $^{25}Mg^{2+}$-related superactivation of energy metabolism requires a minute amount of these ions and works perfectly even in the absence of oxygen (deep tissue hypoxia).

So a desirable application of the above-specified physical/biophysical phenomenon would be the correction for the decline of ATP formation in myocardium tissue suffering from hypoxia of any sort.

To meet these expectations, a novel pharmaceutical nano-tool based on the porphyrin-attached fullerene-C60 "ball" (Porphylleren-MC16 or PMC16) is now proposed [1,2].

Medicinal hypoxia syndromes, i.e. the drug side effects leading to sharp oxygen consumption decrease in mammalian tissues, complicate some anticancer chemotherapeutic procedures. Thus, a doxorubicin (DXR) induced cardiotoxicity relates predominantly to the suppression of the ADP *oxidative phosphorylation* in myocardial mitochondria [3–5]. That means, the reserve ATP regeneration pathway, namely the creatine kinase (CK) directed ADP phosphorylation [6,7], could be chosen as a target for pharmacological impact having an aim to minimize, i.e. to reduce if not even exclude, the DXR side effect in a course of (or prior to) the long-term cytostatic medication.

Being Mg^{2+}-dependent processes, both substrate and oxidative phosphorylation pathways might be activated up to 2.5-fold more efficiently by ultramicro-amounts of $^{25}Mg^{2+}$, *the only magnetic magnesium isotope*, as compared to non-magnetic $^{24}Mg^{2+}$ and $^{26}Mg^{2+}$ isotopes [8]. A simple "endoosmic pressure" is to replace

Abbreviations: DXR, doxorubicin; MNA, 1-methylnicotineamide; CK, creatine kinase; SANS, small angle neutron scattering.

* Corresponding author.
E-mail addresses: rezayat@sina.tums.ac.ir (S.M. Rezayat), sarkar@sina.tums.ac.ir (S. Sarkar), amirshahi@mail.ru, amupwaxu@gmail.com (R.N. Amirshahi), orlova.radiochem@mail.ru (M.A. Orlova), kuznetsov.icp@mail.ru (D.A. Kuznetsov).

0223-5234/$ – see front matter © 2008 Elsevier Masson SAS. All rights reserved.
doi:10.1016/j.ejmech.2008.07.030

one Mg isotope by another (all of them are stable ones) inside the CK active site [9]. This is about *the magnetic isotope effect* of $^{25}Mg^{2+}$ which is now found to be an essential, *overactivating* element in the magnesium-dependent ATP production control [8–11]. It makes a targeted delivery of the above-mentioned magnetic isotope (+5/2 nuclear spin, 0.85 Bohr magnetron magnetic moment, 11% natural abundance) towards a hypoxia damaged cells/tissues a truly important pharmacological task. So the Mg^{2+}-exchanging nanoparticles would be an appropriate tool for such a targeting.

For this purpose, a low toxic ($LD_{50} = 896$ mg/kg, i.v., rats), amphiphilic (430 mg/ml water, pH 7.40), membranotropic and cluster forming 1.8 nm fullerene-C_{60} based particles were now designed [1,2]. This novel medicinal product, which possesses marked cationite properties (Fig. 1), is the iron containing porphyrin monoadduct of a classical buckminster fullerene, *buckminsterfullerene(C_{60})-2-(butadiene-1-yl)-tetra(o-γ-aminobutyryl-o-phthalyl)ferroporphyrin*. Due to a protocol reason, it has been called a "Porphylleren-MC16" or, in brief, PMC16.

One would have at least two hopes for this agent to meet. First, its unique structure may allow the drug to serve as a nanocationite both in vitro and in vivo which is potentially beneficial in terms of "smart release" of magnesium in hypoxia-caused acidosis. Secondly, a porphyrin domain of PMC16 is expected to provide a tissue selective interaction with the heart muscle specific for porphyrin receptors located in mitochondrial membrane of myocardiocytes [12–14]. This would navigate the drug towards the heart in a manner of real targeted delivery. In the latter case, the drug mitochondria intake seems realistic in view of the PMC16 particle size (1.8 nm) [1,2]. The PMC16 pharmacokinetics and the drug–receptor recognition pattern might prove or disprove that. According to a conventional up-to-date biopharmacy/pharmacology glossary, a *medicinal nanoparticle* or *nanomedicine* means a slowly metabolizing xenobiotic of size of a molecule within a nano-scale range (rigid structure, 1.0–50.0 nm) manifested by a marked tropism in biological structures in vivo and in vitro and capable of penetrating the biological barriers (endothelial, blood/brain, cell wall, cell compartment membranes) with a following pharmacological effect to promote [14].

A present work is devoted to biochemical/pharmacological study on [^{25}Mg]PMC16 effects in rat myocardium affected by either the drug (DXR, MNA) induced hypoxia or air oxygen deficit caused hypoxia with respect to cationite properties of the new nanomedicine tested. This is a part of the broader research project pronouncing an aim to develop a novel nanopharmacological approach to prevent and treat the local tissue hypoxia syndromes (including the DXR promoted cardiotoxicity side effect) by a targeted delivery of $^{25}Mg^{2+}$ cations towards the heart muscle using a porphyrinic-fullerene nanoparticles as the membranotropic Mg^{2+}-releasing carriers.

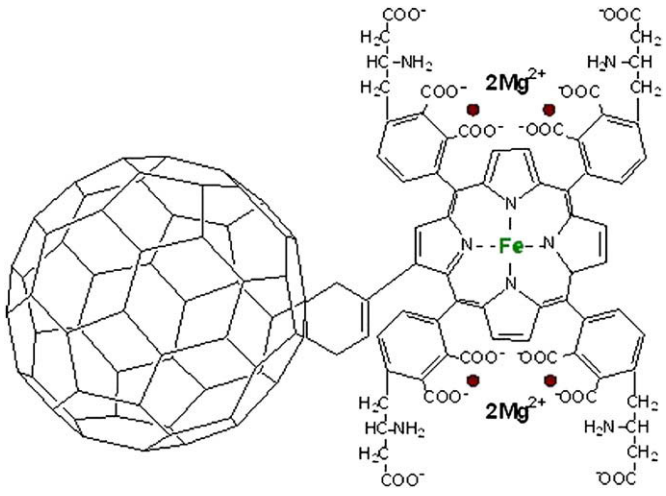

Fig. 1. The PMC16 nanoparticle structure.

2. Materials and methods

2.1. Reagents

DXR, MNA, ATP, ADP, phosphocreatine, creatine, $MgCl_2$, sucrose, all of analytical grade, were purchased from Merck Corp. USA. All organic solvents used were kindly supplied by Bio-Rad, Russia. *Pure magnesium isotopes* were received in a chloride form (96.8% isotopic purity, A grade) from Obninsk Radiochemical Center, Russia. The very same supplier was also responsible for the following radioactive materials provided: $^{59}FeCl_2$ (A grade, 910–960 Ci/mmol specific activity), sodium [^{32}P]orthophosphate (A grade, 600–700 Ci/mmol) and [^{32}P]phosphocreatine (A grade, 280–320 Ci/mmol) were used. Creatine kinase (60–80 U/mg protein), nuclease S (100–120 U/mg protein) and RNase A (100–140 U/mg protein) were purchased from Worthington Corp., USA. Fullerene-C_{60} was purchased from Lachema Corp. (Czech Republic).

2.2. Animals

Wistar Albino Glaxo (WAG/Sto2J strain) male healthy adult rats (180–220 g) used were kept under a standard vitaminized diet, starving for 24 h prior to each one of the test conducted. Three animals per one experimental point with following 5–6 repetitions of every measurement were taken as a rule.

2.3. Hypoxia experimental models

The following in vivo experimental hypoxia models were employed:

(1) Medicinal hypoxia syndrome A (1-methylnicotineamide (MNA), 10–20 mg/kg i.v. once per 24 h);
(2) Medicinal hypoxia syndrome B (DXR 60–80 mg/kg i.v. once per 24 h);
(3) The oxygen-depleted inhalation model (10–20 day long exposition of rats to the artificial gas mixture to breath with 12–16% oxygen/84–88% nitrogen, v/v).

2.4. Isolation of cell compartments

To isolate cell organelle (nuclei, cell wall membranes, mitochondria, cytosol), the heart tissue homogenate was conventionally fractionated by the differential ultracentrifugation in 800 g/12,000 g/35,000 g/125,000 g regime using the Beckman Spinco L5-65B Ultracentrifuge, SW27.1 rotor [15,16]. Scalar 0.8–2.0 M sucrose gradients were applied to isolate and purify the mitochondrial membrane fragments (SW 27.5, 110,000 rpm, 2 h) after the osmotic shock promoted decomposition of organelles and their nuclease S/RNase A treatment [17]. Protein measurements were performed by a routine Bradford colorimetric method [18]. When needed, protein preparations were concentrated on Amicon Diaflo Y5.0 membranes at 800 psi.

2.5. Isotope analysis

^{59}Fe (γ-emitter) and ^{32}P (β-emitter) quantitative radioactivity measurements were conducted in the dioxane LKB scintillation counting fluids using the LKB SK260 and the Wallac 410B liquid scintillation counters, respectively.

For the ^{59}Fe-related autoradiography of the organelles isolated, Fuji RX40 films were employed along with the Farrand XL30

transmission electron microscopy unit with a consequent negative track analysis [19].

Estimations of magnesium stable isotopes (^{25}Mg, ^{24}Mg, ^{26}Mg) were carried out in the Olivetti Prism DL600 isotope mass spectrometer suitable for studies on heterogenous samples of biological origin [8,10]. For the PMC16 saturation with $^{25}Mg^{2+}$ cations, our original electro-osmotic technique has been applied [1,2].

2.6. Preparation of PMC16 $[^{25}Mg^{2+}]_4$ nanoparticles

The aiming compound (Porphylleren-MC16 or PMC16) prepared by the following method is exemplified in Scheme 1, steps 1–10.

First, a diethyl phthalate is to be silicomethylated by trimethylsilicochloride in the presence of butyllithium catalyst with a formation of diethyl-3-(trimethylsilyl)phthalate (Product II, step 1). The latter one is then transformed into diethyl-3-formyl-6-(trimethylsilyl)phthalate (Product III) by the oxidation of Product II in the presence of the same mentioned catalyst and dimethylformamide (step 2). Product III is then monobromated by *N*-bromosuccinimide in the presence of tetrabutylammonium fluoride so diethyl-6-bromo-3-formylphthalate (Product IV) formed as a result (step 3). Next, Product IV is to be condensated with pyrrol in the presence of 2,3-dichloro-5,6-dicyano-1,4-benzoquinone (DDQ) which leads to the formation of Product V, the first obtained porphyrin structure (step 4). Then Product V

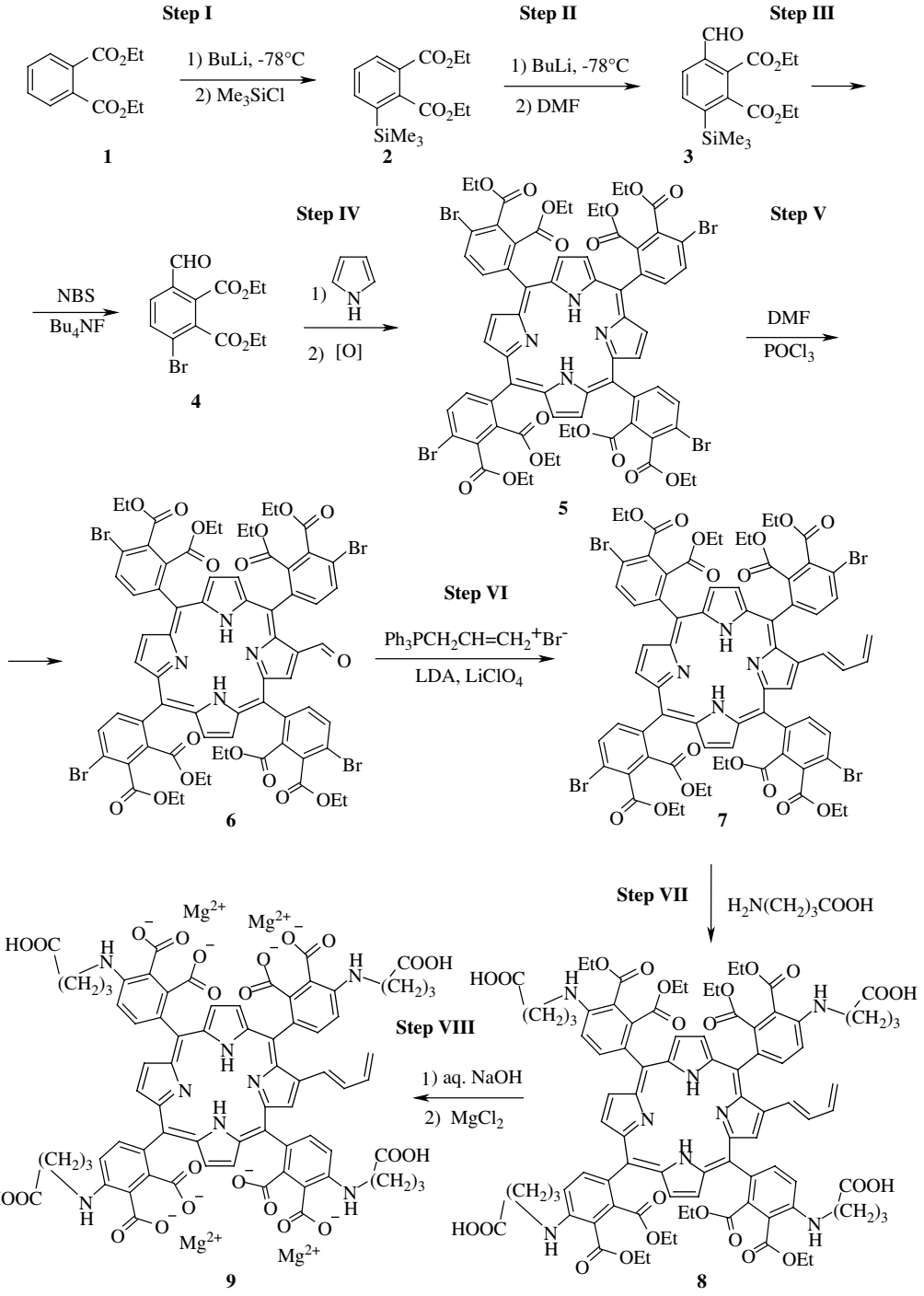

Scheme 1. The PMC16 synthesis route's key steps.

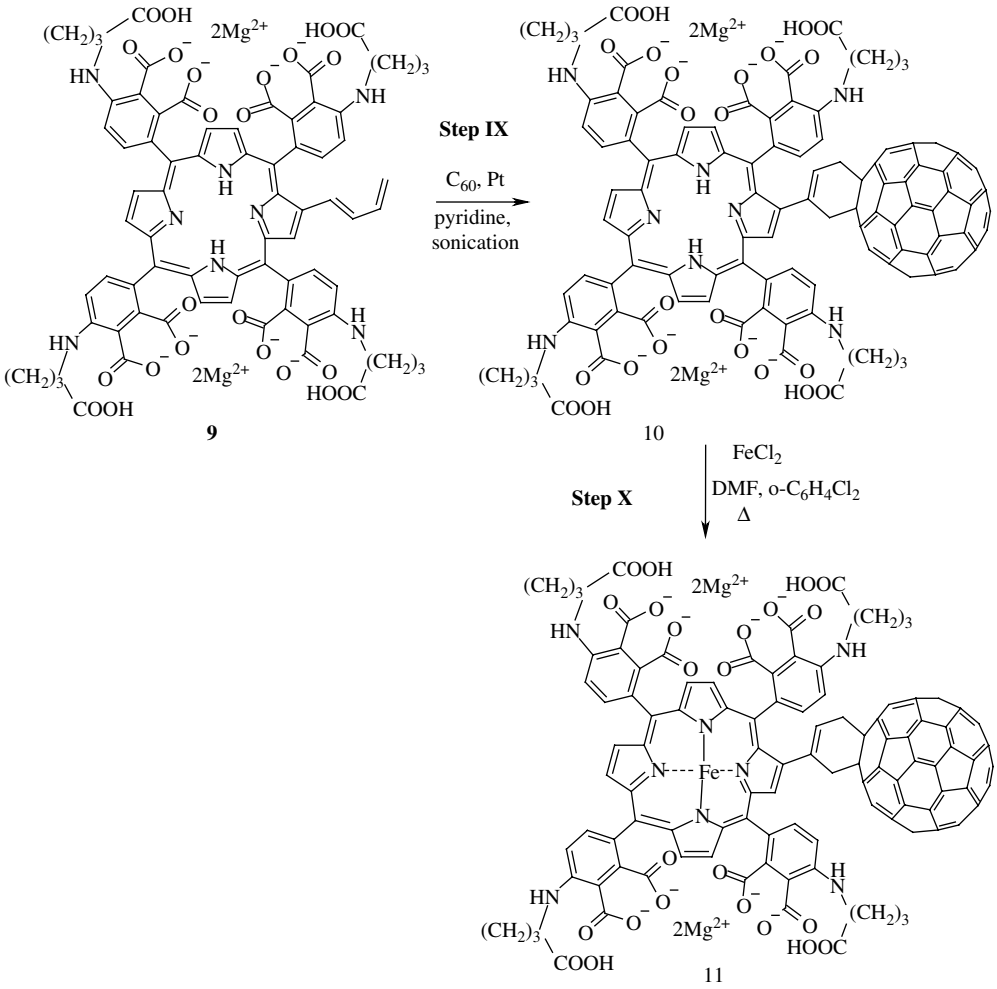

Scheme 1. (*continued*).

transforms into Product VI (step 5) in the presence of dimethylformamide and $POCl_3$.

Consequently, Product VI transforms into Product VII by the one-step combined treatment with lithium diisopropylamide (LDA) and lithium perchlorate (step 6). Gamma-aminobutyric acid is to induce the transformation of Product VII into Product VIII as indicated in Scheme 1 (step 7). Simple addition of NaOH and $MgCl_2$ transforms Product VIII into Product IX which, in turn, then transforms into the fullerene porphyrin adduct by the treatment with a pure C_{60}-fullerene, Pt catalyst (powder suspension), here a simple pyridine sonication is involved. Eventually, the final PMC16 nanostructure is to be formed from Product X by incubation (combined simultaneous treatment) with $FeCl_2$, *o*-dichlorobenzene and dimethylformamide (step 10).

PMC16 "loading" with $^{25}Mg^{2+}$ cations (saturation, PMC16[Mg^{2+}]$_4$) is done according to a following procedure. Up to 600–800 mg of PMC16 is dissolved in 1.0 ml mixture of pyridine:CS_2:chloroform (1:2:7) at room temperature. Then 4 volumes of 2.5 M solution of pure $^{25}MgCl_2$ (98.6% isotopic purity) in 0.2 M NaOH has been added to the PMC16-containing organic mixture. After 30 min of extensive shaking (22–25 °C), the water-soluble phase was separated by centrifugation at 15,000 rpm, 20 min, 22 °C, carefully collected and then lyophilized or evaporated with a following mass spec and atomic absorption spec control.

The remaining organic phase was repeatedly (2–3×) subjected to Mg^{2+} alkaline–water extraction, the organic phase-containing $^{25}MgCl_2$ traces were then re-utilized using the fast rotor evaporation and a consequent dissolving in 10 mM sodium-phosphate (pH 9.60) buffer containing 15 mM EDTA. The very same way to concentrate the resulted [^{25}Mg]PMC16 was applied to the first alkaline–water extraction run.

Noteworthy, the diethyl phthalate was initiated by butyllithium at −78 °C followed by the quenching of carbanion with trimethylsilyl chloride. The resulting diethyl-3-(trimethylsilyl)-phthalate was subsequently treated with butyllithium and DMF (dimethylformamide) leading to the corresponding benzaldehyde. Its reaction with *N*-bromosuccinimide in the presence of Bu_4NF gave a diethyl-6-bromo-3-formylphthalate which was a final precursor for the substituted porphyrin synthesis. Then 5,10,15,20-tetrakis[4-bromo-2,3-bis(ethoxycarbonyl)phenyl]-21*H*,23*H*-porphine was synthesized by the routine Lewis acid-catalyzed condensation of this precursor with pyrrol followed by treatment with DDQ according to the standard Lindsay procedure (Scheme 1, steps 1–4).

Another peculiarity of this synthetic route to stress out (Scheme 1, steps 5–10) is that the Vilsmeier–Haak formylation of the porphyrin obtained was carried out conventionally in the DMF/$POCl_3$ mixture with a following promotion of the Witting reaction conducted with allyltriphenyl-phosphonium bromide yielding butadienyl-substituted porphyrin F. A classical copper-catalyzed reaction of the latter with an excess of gamma-aminobutyric acid then resulted in the formation of 2-(buta-1,3-dienyl)-5,10,15,20-tetrakis[4-(3-carboxypropylamino)-2,3-bis(ethoxycarbonyl)phenyl]-21*H*,23*H*-porphine. An alkaline hydrolysis of this product, along with a magnesium chloride induced cation

metathesis and a reaction between the butadienyl moiety and the C_{60}-fullerene combined with metalation of the porphyrin core with $FeCl_2$ were then completed in the eventual formation of the goal product [1].

To identify the CS_2-extracted resulting product, the fast atom bombardment (FAB) mass spectra were registered in Varian GT800 LC–MS machine and then processed in the HP6100-J2A analytical unit using a Sigma Delta Chem AX2000 data base. In addition, a combined MALDI (matrix assisted laser desorption/ionization) and FI/FD (field ionization/field desorption) techniques were also employed to identify the product structure using the MALDI-QX90A/Finnigan Matt and the MS400/Olivetti tools, respectively, with a following automated spectra resolution in the above-mentioned HP analytical unit but applying another data base software, *LabRun-2002* [1,12,14,20]. For pharmacokinetic and autoradiographic studies, special samples of [^{59}Fe]PMC16 (280–320 Ci/mmol) were obtained using the A grade $^{59}FeCl_2$ (910–960 Ci/mmol, Obninsk Radiochemical Center, Russia) as a precursor.

2.7. PMC16 measurement in biological material

A pure CS_2 was applied as a universal PMC16 extragent in studies on lyophilized samples of either isolated cell compartments or a crude heart tissue homogenates, 8.0–12.0 w/v, 22–25 °C, extensive shaking. The resulting extracts were repeatedly treated with 7.5 vols pyridine (3–5×); all post-extraction pyridine portions were then collected, combined, and concentrated in rotor evaporizer. A 15–20 μl aliquots of the PMC16-containing concentrated extracts was fractionated by HPLC using a CosmoSil 5-PBB (the PentaBromBenzene-modified silica gel suitable for separation of porphyrinic fullerenes), 20 × 250 mm column at 22 °C, 1200–1500 psi, 10 ml/min, with a pure 1,2,4-trichlorobenzene as a mobile phase [20]. The final PMC16 quantification was performed planigraphically with an automatized correction for molar extinction indexes once the elution profile got recorded by absorption at 180, 210, 320, and 470 nm in Perkin Elmer 266QL HPLC Analytical System.

2.8. The PMC16 in vitro tests

For the drug nano-size measurements as well as for the pH-dependent PMC16 cluster formation direct monitoring, a two-dimensional arrays of nanoparticles and their conglomerates were registered by the atomic force microscopy in the Zelenograd-ERA M3 (Russia) AFM system [20]. Apart from AFM, the PMC16 cluster sizes were also estimated by gel filtration on Sephadexes G10, G15 and G50 within an eluent pH range of 5.0–9.5 [1]. The PMC16-related Mg^{2+} release kinetics has been simultaneously tested, within the same pH range, by evaluation of the Mg/Fe ratios using a routine flame atomic absorption spectrophotometry method (DX800-B6 Carl Zeiss AAS, Carl Zeiss Jana). SANS spectra of PMC16 monomers and dimers were registered and analysed in SANS 2TD accelerator at the International Nuclear Research Institute, Dubna, Russia, with a kind technical assistance provided by Dr. M.N. Osmolov.

2.9. Biomaterial morphology tests

For morphological tracing of PMC16 particles inside the organelle membranes, a metal-chelating iron response AFM toolbox along with a simple imaging AFM biological version [14,20] was employed. The in situ morphology of mitochondria in myocardiocytes was observed by a routine transmission electron microscopy using a Pt contrasting coating [16]. A laser contrast confocal microscopy was additionally employed using a Nanofinder-S16E (Nanofinder Co., Russia) technology as described by the manufacturer [21].

2.10. ATP synthesis rate measurements

Once mitochondria were isolated, they were rapidly submitted to the Triton X-100 treatment (2.0%, v/v, +4 °C, 2 h, 10 mM Tris–HCl pH 7.45) with a following extraction of a total pool of the low molecular mass compounds by the addition of 10 vols ice-cold acetone. The resulting acetone-soluble material was then fractionated by our original HPLC procedure (ODS-S5CN stationary phase/10–60% linear pyridine gradient mobile phase, Altex 1800 15 × 280 mm column, 22 °C, 2000 psi, Gilson W100 UV-detecting HPLC system) in order to get both ATP/ADP ratio values and the ATP production rate estimated as γ-[^{32}P]ATP cpm/mg protein [22]. In all in vivo [^{32}P]orthophosphate ATP labelling tests, animals were sacrificed in 20–180 min time interval after a single 80–100 mCi/kg i.v. injection of the label used. A CK activity was measured as described earlier [8].

2.11. Heart muscle oxygen consumption measurements

Both heart tissue homogenates and the isolated mitochondrial samples were subjects for [O_2] and [ΔH^+] parameters' estimation. A BioRad OxyAnalyser SJ80 has been employed for the tissue/mitochondrial oxygen consumption tests. In these studies, the phosphorescence-based oxygen analyzer was superior to the conventional oxygen electrode system in that it provided an accurate, sensitive and reproducible quantitation of [O_2]. Measurements in this study were performed over periods up to 60 min, thus ensuring cell viability. Measurements on re-aerated suspensions showed that the probe was stable and did not interfere with cell function. Stoichiometric titration of oxygen with ascorbate in the presence of ascorbate oxidase (2 ascorbate + O_2 → 2 dehydroascorbate + 2 H_2O) was done as described [23]. The tissue free protons' content was potentiometrically evaluated in homogenates using a Pt/Ar microelectrode in an extensively aerated cell coupled with the [O_2] detecting unit [23,24].

2.12. Pharmacokinetics and pharmacodynamics

All nine major pharmacokinetics parameters along with 12 additional ones (Table 1) were estimated by the standard

Table 1
The [Mg]PMC16 pharmacokinetics in rat

$T_{1/2} = 9.0$ h	$C_0 = 62$ μg/ml
$T_{max} = 2.5$ h	$C_{max} = 260 \pm 83$ ng/ml
Cl = 32 ± 4 ml/min/kg	$V_P = 16.2$ ml/kg
$k = 0.685$	$V_C = 12.4$ ml
	$V_1 = 0.08$ ml
Renal excretion	28 ± 4.3%
Hepatic excretion(*metabolization*)	16 ± 4.0%
Plasma proteins binding	1.2 ± 0.3%
Blood cells uptake	
Lymphocytes	28.6 ± 5.5%
Erythrocytes	8.0 ± 3.2%
Tissue-specific accumulation	
Myocardium	18.4 ± 3.40%
Brain	0.6 ± 0.02%
Urine-eliminating PMC16 metabolites (258 ± 4.0 μg/ml)	
Alanyl-depleted derivatives	56.4 ± 8.7%
Deacetylated derivatives	27.0 ± 6.1%
Cyclohexyl-C_{60}	16.2 ± 3.3%
PMC16 urine content	462 ± 11 μg/ml
C_{60} urine content	2.9 ± 0.1 μg/ml

Single 20 mg/kg i.v. injection ($M \pm$ SEM, $n = 6$) 24 h monitoring presented.

procedures specified clearly in Section 3. To identify/quantify the PMC16 and its metabolites in any biomaterial tested (urine, blood cells and plasma, tissue homogenates, cell compartments), a lyophilized CS_2/acetone extracts were used for chromato-mass spectrometry procedure (GC–FAB/MS, LC–MALDI, FI/FD–MS) [1,12,14].

This technique allows to detect even the water-insoluble PMC16 metabolites including a pure C_{60} [1].

Blood plasma transferrin, hemoglobin, myoglobin and liver ferritin isolation shots were carried out using a fast double immunoprecipitation technique, Bio-Rad 1167JS Analytical Kit, as recommended by the manufacturer [25].

Ficoll mini-column preparative fractionation of cells was applied to erythrocytes and lymphocytes isolation [26].

A possible sorption of the drug tested on blood plasma proteins has been studied using the [^{59}Fe]PMC16 species according to Ref. [27].

All the results obtained were statistically treated with respect to a classical two-compartment drug distribution model [28,29].

2.13. Statistics

A conventional non-parametric statistical treatment (for "*n*" equal to 6 or lower) was performed using the Sigma Biostat A6 software package to evaluate the significance of experiment/control differences. A Penmann–Dalbreaux approximation technique has then been employed once the standard error of the mean (SEM) values were found to be not higher than 6.5% of the mean (0.020–0.065 M limit range) whatever pair compared. To manage this, the HP LabRun-06 software operating graph-design algorithm has been processed in the HP6100-J2A Analytical Unit to perfectionize all graphics [19,20,29].

3. Results and discussion

A not-too-long lasting history of the medicinal use of fullerene-based nanoparticles includes a clear indication of their very low acute toxicity [20,30] as well as a variety of data that reveal the fullerene derivatives' anti-malignant [31], anti-viral [32] and bacteriostatic [33] properties. It would be safe to say, however, that the main stream trends in a modern fullerenes' nanopharmacology research deal with the targeted drug delivery problem due to marked capabilities of these membranotropic nanoagents to serve as specific carriers for organic/bioorganic pharmaceuticals [34,35]. As for a tissue targeting mechanism, magnetic and immunovectoring navigation paths *alone* were tested so far with respect to this very peculiar family of nanomedicines [20,36].

Let us remind that the latter term (*medicinal nanoparticles*, *nanomedicines*) stands for the biologically active nano-size synthetic structures capable of moving across the main types of biological barriers with further targeting towards a certain receptor(s) inside or outside the cell and without being instantly destructed by surrounding enzymes [14,37–42].

To the best of our knowledge, no research but ours was in fact devoted to the C_{60}-fullerene derivatives' *cationite* activity [1,2]. On the other hand, this is exactly the activity needed to provide a delivery of $^{25}Mg^{2+}$ cations towards a hypoxia suffering cells and tissues. According to our basic standpoint, a targeted delivery mentioned may help to compensate the hypoxia-caused ATP losses owing to a known ^{25}Mg-related overactivation of both oxidative and substrate ADP phosphorylation paths of the ATP synthesis in a cell [8–11].

As seen from our data presented in Figs. 1 and 2, the PMC16 possesses an essential Mg^{2+}-carrying cationite potential. Noteworthy, the product may act as a so-called smart nanoparticle being capable of releasing magnesium in response to the pH acidic shift

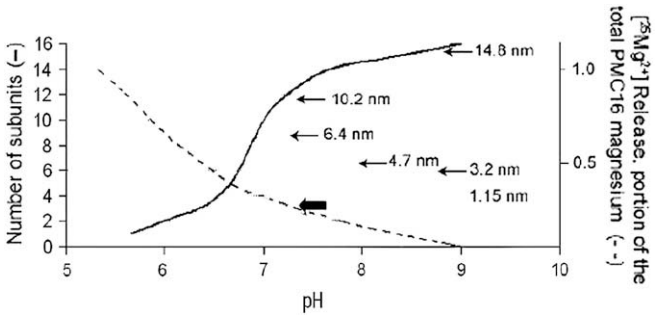

Fig. 2. PMC16 cationite properties and nanocluster formation as a function of pH. Big arrow shows the normal homeostasis edge point.

(Fig. 2). At the same time, the PMC16 cluster formation is also found to be a function of pH (Figs. 2–4). These findings look attractive in the light of the myocardial hypoxia molecular pathogenesis data, according to which a tissue acidosis is a direct and natural metabolic consequence of the hypoxia of any sort [2,7,11,16]. So the acidosis induced release of $^{25}Mg^{2+}$ is what we may expect in case of the [^{25}Mg]PMC16 in vivo administration. The amphiphilic character of this agent [1,2] is also in favor of such expectations since the ambivalent solubility of the drug correlates normally with its membranotropic properties [14,17,20]. And, indeed, the PMC16 biomembrane uptake has been eventually found (Fig. 5). The AFM technical approach we used to obtain these data [14,20] is a late modification of the most efficient earlier developments performed in biophysical studies on living cells and their compartments [39–42]. Besides, a non-allergic and anti-inflammation properties of most fullerene derivatives ever tested [37,38] as well as their generally high level of "biocompatibility" [39] make PMC16 suitable for the in vivo safety and pharmacological activity studies.

Both morphological (Fig. 6) and biochemical (Fig. 7) patterns show a clear and positive effect of [^{25}Mg]PMC16 on the hypoxia promoted myocardial cell energy metabolism disorders. Additionally, this has been proven by a high level of synergism manifested in the [^{25}Mg]PMC16 hypoxia treated cases, i.e. by a synergism between the CK activity, ATP production rate, magnesium isotopes contents in the heart mitochondria, myocardial O_2 consumption and the tissue acidosis ([$\Delta H\uparrow$]) degree (Figs. 8 and 9).

The MNA-induced tissue hypoxia comes with inhibitor's complete, selective and irreversible suppression of the ADP oxidative phosphorylation in mitochondria as long as this agent is the NAD/NADP precursing antimetabolite [8,9]. Unlike MNA, DXR provides much slighter inhibitory effect towards ATP synthase and cytochrome oxidase in mitochondria [4,5] which makes both drugs comparable to each other in terms of the depth of medicinal hypoxia induced. Whatever hypoxia model tested, the [^{25}Mg]PMC16 prophylactic or corrective use look at an efficient way to either prevent or correct the ATP-depleting metabolic disorders (Figs. 6–9) and, hence, to protect the heart muscle in general.

Another remarkable peculiarity of PMC16 nanoparticles is a fact of their days-long lasting retaining in the heart tissue (Fig. 10) and, particularly, inside the heart mitochondrial membranes (Figs. 11 and 12E). In our opinion, the most probable explanation for this phenomenon is an existence of the PMC16 high-affinity protein receptor in these membranes, i.e. a presence of the signaling protein responsible for a selective drug–protein recognition. A mere protein signaling function of that type is known for a number of porphyrin metabolites [12–14,16].

A total lack of the PMC16 long-lasting "trapping" observed in tests conducted on several other tissues (liver, lungs, kidneys, skeletal muscles) is in a good accordance with an above stated assumption (Fig. 12). A relatively fast systemic clearance of this

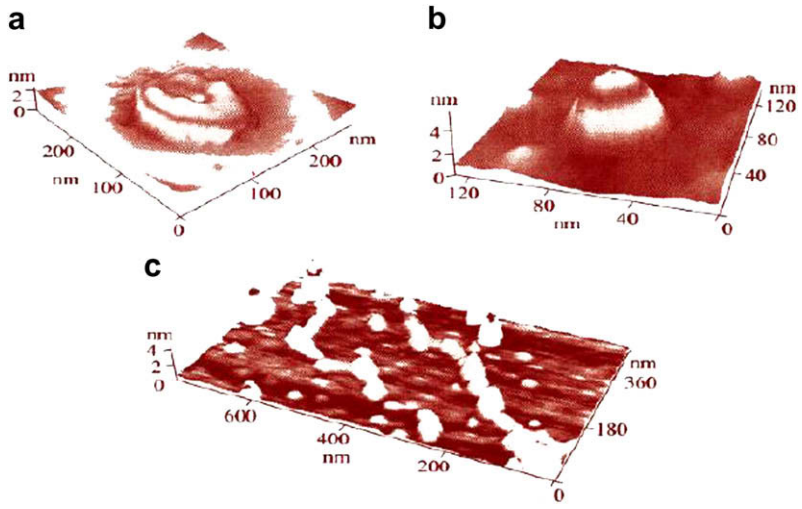

Fig. 3. Laser contrast and atomic force microscopy. PMC16 nanoclusters immobilized on acetyl cellulose membrane [40,44]. (a) LCM, pH = 7.00; (b) LCM, pH = 8.40; (c) AFM, pH = 8.80.

nanomedicine along with a nearly perfect tissue clearance estimated for numerous PMC16 "non-trapping" tissues listed above seems an additional argument to prove a high potential of PMC16 for the heart-selective $^{25}Mg^{2+}$ targeted delivery (Figs. 13 and 14).

The heart muscle tissue manifests its high capability to retain the drug non-metabolized molecules for longer than a week. After a single i.v. injection (20–30 mg/kg), about 18.0% of the whole amount of the drug injected remains in myocardium for 12 days. At the same time, there is no sign of tissue-specific accumulation of this drug (no 24 h or longer retaining) in skeletal muscles, kidneys, lungs and liver (Figs. 10–12).

Considering the isolation of purified receptor a non-urgent although important task for further studies, we may gain, nevertheless, a rather obvious advantage of the very fact of the heart muscle specific PMC16 reception.

Once we do have a reliable information on the drug receptor presence in the heart (Figs. 10–12), then, *the receptor dependent targeted drug delivery* should be expected. That means, extra low drug doses multiple administration scheme may lead to accumulation of the drug molecules exclusively inside the so-called drug-specific receptor-rich body compartments whereas the rest of the whole organism may remain practically drug-free due to a normal elimination mechanism.

This statement has been proven indeed by the heart muscle targeted delivery of [^{25}Mg]PMC16 which we have reached by developing of a special scheme of the multiple long-term administration of low drug doses. In Fig. 13, a true efficiency of this scheme (0.4 mg/kg, i.v. [10 days] – 0.2 mg/kg, i.v. [6 days] – 0.1 mg/kg, i.v. – …up to 24 days monitored) is presented. The scheme proposed comes from our understanding of pharmacological meaning of the PMC16 heart muscle specific reception. Particularly, this scheme provides a *saturation* of majority if not of all of the heart-located PMC16-specific receptors in case of the gradual administration of drug doses *minimal but enough* to get this saturation reached. Meanwhile, all other receptor-lacking body compartments are not in a position to retain the drug as long as its concentration is below an accumulation-required elimination limit. That's the extra low doses are for. All together, this creates a unique condition for the heart drug targeting even *without any effort to manage the artificially designed targeted delivery path* like, for example, the external magnetic field navigation or the antibody involving liposome drug delivery.

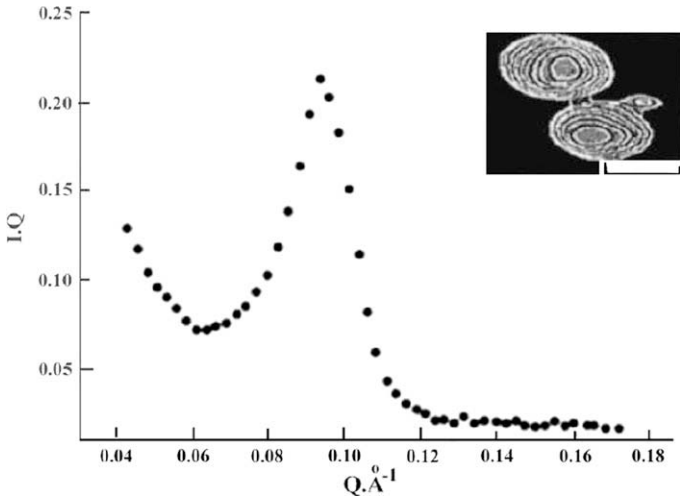

Fig. 4. Small angle neutron scattering image of the PMC16 mono/dimer, pH 6.50 (scale bar: 1.0 nm).

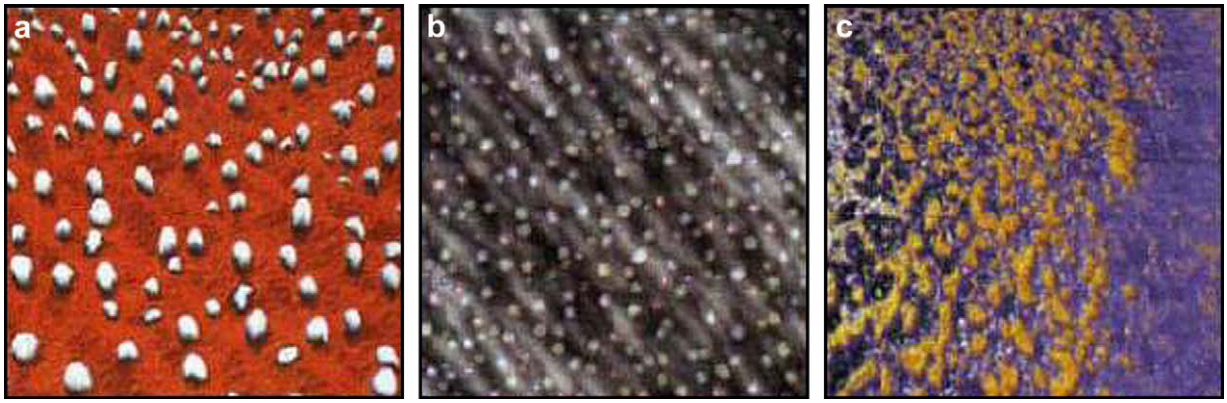

Fig. 5. The PMC16 nanoparticles/clusters atomic force micrographs: (a) suspension, 400 mg/ml 1.5 mM K_2HPO_4 (pH 10.0); 10 nm scale bar; (b) diaflo YM 1.0 membrane remained pellets, 400 mg/ml 1.5 mM K_2HPO_4 (pH 9.0) suspension used; 100 nm scale bar; (c) rat myocardial mitochondria membrane lipid layer. 0.1 LD_{50} PMC16, 10 h → 0.8 LD_{50} DXR, 10 h; 50 nm scale bar.

In a contrast to these known drug delivery paths [42–44], the porphyrin tissue receptors docking way look far more preferable due to ability of 1.8 nm PMC16 particles to intervene the cell (Figs. 6, 11, and 12) for further possible coupling with corresponding affinity proteins located in mitochondrial membranes of myocardiocytes [6,14,16].

Noteworthy, the only reason why these low doses of PMC16 are enough to promote an essential pharmacological effect in the hypoxia damaged myocardial cells, i.e. to promote a marked activation of the ATP synthesis, is the efficient delivery of ^{25}Mg isotopes known as the universal ATP production *overactivating agents* [8–11]. So despite a low tissue drug concentration, the energy metabolism rehabilitation is to be taken care of by a very small amount of an *extremely active* ATP regeneration promoter which is a magnetic magnesium isotope of ^{25}Mg. As a cationite carrier for magnesium, the PMC16 is certainly a right nano-tool to provide a proper pharmacological application of the $^{25}Mg^{2+}$-related magnetic isotope effect. Thus, being capable for a tissue-specific targeting, this tool allows not to waste paramagnetic all over the whole organism which helps to avoid the unpredictable side effects dealing with ATP hyperproduction in cells apart from myocardiocytes and lymphocytes. Other advantages of the PMC16 medicinal use, as seen from everything stated above, are the drug smart magnesium release, a long-term drug–receptor retaining in target tissue, and a high biological activity of minute amounts of $^{25}Mg^{2+}$ delivered.

These and related statements are, as a matter of fact, supported by a complex but positive correlation revealed between the heart tissue ^{25}Mg content values and the tissue respiration parameters ([ATP], [ATP]/[ADP], Y/Y_o; [ΔO_2], [ΔH^+]) measured in both DXR- and MNA-induced hypoxia chronic experiments (Figs. 8 and 9).

The data presented may serve as a background for a new nanopharmacological approach to prevent and correct a number of

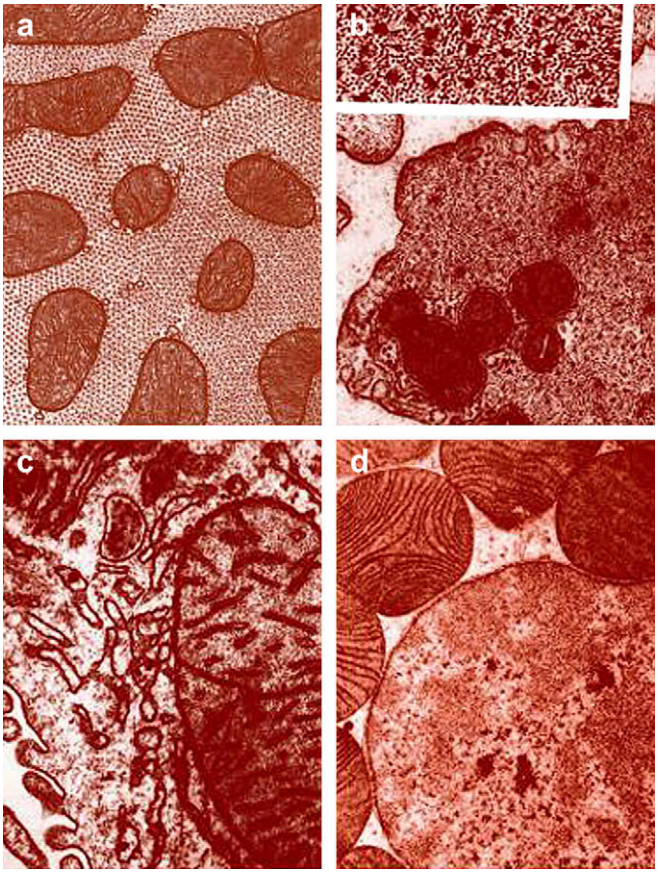

Fig. 6. Electron transmitting microphotograms of the rat myocardiocytic perinuclear areas. A,C: PMC16-related hypoxia preventing effect (30 mg/kg [^{25}Mg]PMC16, i.v. → 12 h → 20 mg/kg MNA, i.v. → 12 h → test); B: MNA hypoxia model (20 mg/kg MNA → 12 h → test); D: control (healthy intact rat tissue).

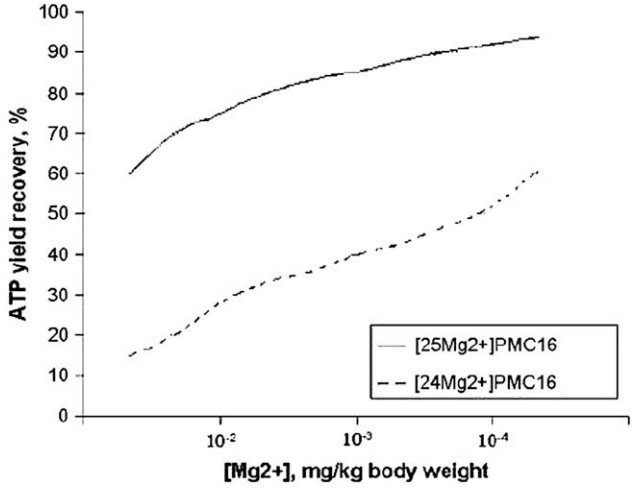

Fig. 7. The effect of a PMC16-targeted delivery of Mg^{2+} on the doxorubicin pre-suppressed ATP production in rat myocardium (0.8 LD_{50} DXR i.v., 6 h → PMC16, i.v., 6 h).

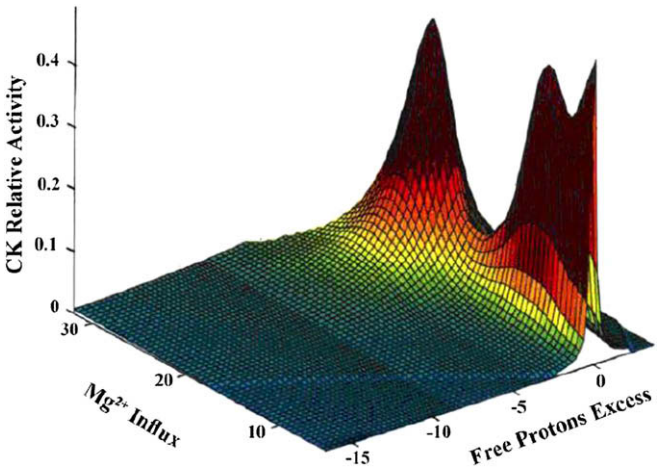

Fig. 8. Synergism of the mitochondrial matrix CK activity, PMC16-related magnesium cations influx and the free protons excess degree. Isolated rat myocardial mitochondria pre-treated with 0.25 DL_{50} PMC16.

myocardial hypoxic disorders. The way proposed includes the heart muscle targeted delivery of magnetic $^{25}Mg^{2+}$ isotope carrying by membranotropic cation-exchanging fullerene-based nanoparticles, PMC16. The heart drug targeting depends on the PMC16 tissue-specific reception while the magnesium release is just a response to hypoxia-caused metabolic acidosis. That makes an agent a tested "smart medicinal nanoparticle". All findings listed look promising and require further extensive studies.

As per the pharmacokinetics/pharmacodynamics patterns, even though they may look guite self-sufficient (Table 1; Figs. 10–18), some of them might be pointed out.

Thus, the blood plasma drug concentration dynamics (20 mg/kg [^{25}Mg]PMC16, i.v.) has been started to investigate, 10 min after a single injection. In *s* semi-logarithmic coordinate (Fig. 14), a concentration time dependence ($C = f(T)$) is found to be describable by two consequent exponential functions. That means, we are dealing with a classical two-compartment drug distribution model [27–29].

The routine pharmacokinetics analysis reveals the following key parametric values, which are all listed in Table 1.

$$T_{1/2} = 9.0\ \text{h};\ T_{\max} = 2.5\ \text{h};\ C_{\max} = 260\ \text{ng/ml}.$$

$$\text{Cl} = D/S = 32\ \text{ml/min/kg}$$

where D – dose, S – square under pharamacological curve. V_p stands for a drug distribution volume which is a ratio of a total clearance (C1) to the drug elimination constant (k), i.e. to the constant of the rate of a drug blood plasma concentration decrease registered at the steady state point.

$$V_p = 16\ \text{ml/kg};\ k = 0.685 \quad V_p = \text{Cl}/k = D/(k \times S)$$

Besides, $V_p = C_b/C_{p1}$ where C_b – a total content of the drug in a whole body, C_{p1} – drug plasma concentration.

$C_o = 62$ μg;/ml, this is the drug concentration which could be reached in the very moment of its injection.

$V_c = 12.4$ ml, $T_{1/2} = k(V_c/\text{Cl})$ which is actual for the steady state moment.

Thus, V_c is a drug distribution volume at the steady state condition. That is, this is a volume in which the drug is supposed to be distributed once the steady state status is in fact reached if its concentration in this volume would become the same as in plasma or in a whole blood of the animal [29].

$V_1 = D/C_o = 0.08$ ml, V_1 – the initial distribution volume (a central compartment volume).

So if we would neglect the drug concentration measurement in an early time step after the injection (10–30 min), the resulting PMC16 pharmacokinetic model would be mistakenly defined as a single compartment one. We escaped such an error by direct detailing of the very first steps of the drug concentration dynamics (Figs. 14 and 15). The error mentioned would come to about 10–12% by clearance alone [27].

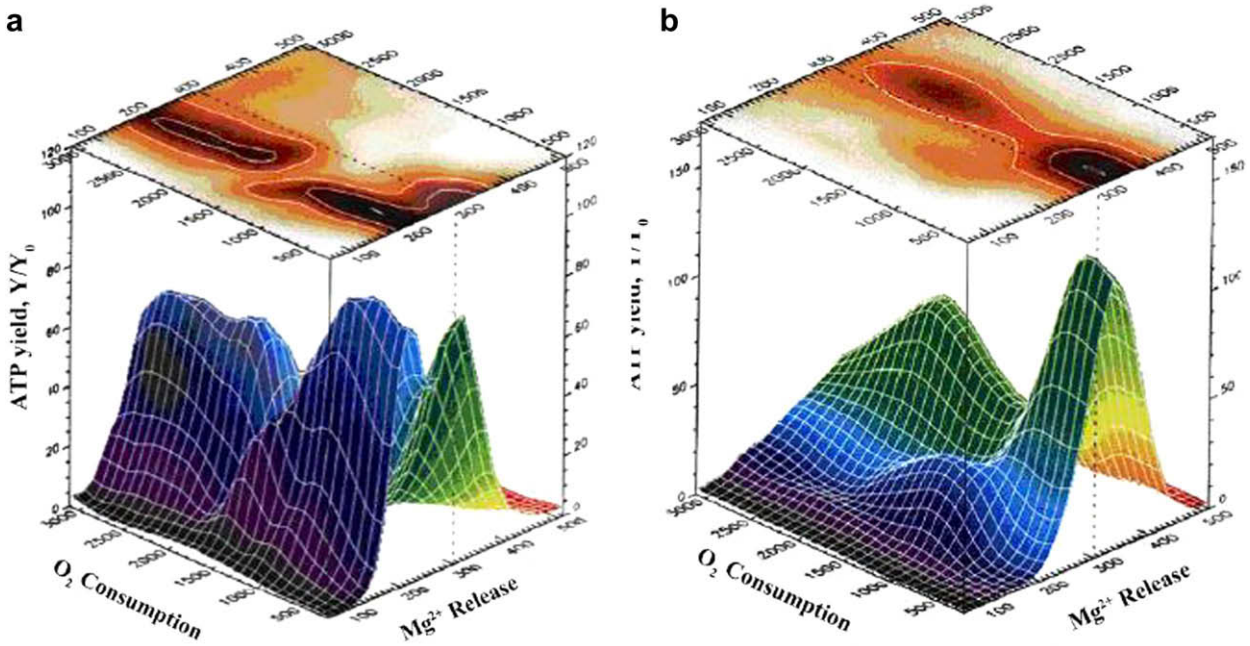

Fig. 9. Synergism of the ATP yield, oxygen consumption and the PMC16-related Mg^{2+} release in the rat heart muscle tissue (30 mg/kg PMC16, i.v., 12 h exposition). A: zero spin magnesium test; B: magnetic magnesium test.

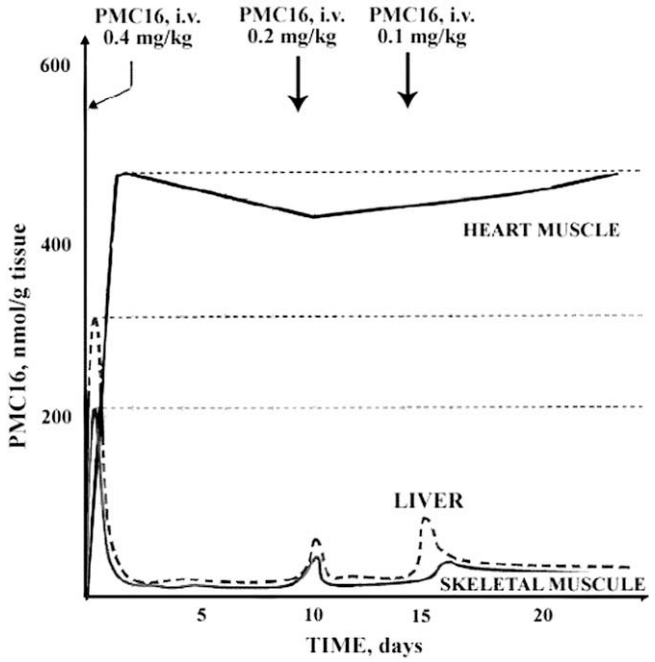

Fig. 10. A highly selective targeting of PMC16 nanoparticles towards the rat heart muscle in a course of the long-term administration of an extra low drug dosage.

The differences between the drug distribution levels within central and distant compartments are important to be tested in the saturation doses' estimation.

The drug distribution volume (V_p) does not necessarily correspond to some real volume. V_p is just a volume needed for an equal, homogenous, distribution of the drug in the very same concentration as in plasma or in total blood. The PMC16 is found to posses almost a zero affinity towards the plasma proteins (PP binding degree = 1.2%). Its renal excretion level is 28% and hepatic excretion (metabolizing extent) is 16%.

The PMC16 blood cell in vivo uptake is up to 36% (24 h monitoring): 28% in lymphocytes and 8% in erythrocytes.

The urine excreting nine metabolites is found to have the following ones (Table 1; Fig. 16):

Alanyl-depleted PMC16 species – 56%,
Deacylated PMC16 species – 28%,
Cyclohexyl-C_{60} – 16%.

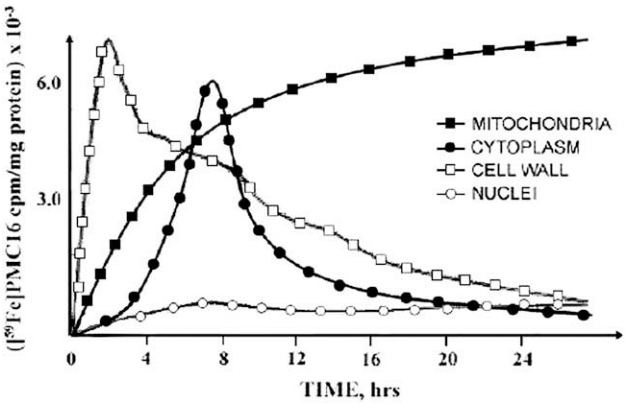

Fig. 11. The heart muscle cell compartment retaining distribution of [^{59}Fe]PMC16 caused by a single i.v. administration in rats (30 mg/kg, 470–520 Ci/kg).

It should be stressed out that the PMC16 shows a marked tissue-specific accumulation exclusively in the heart muscle (18.4%) and in the brain (0.6%). This indicates to the above-discussed drug reception mechanism and, not less importantly, perhaps to the blood–brain barrier penetration abilities as well. Looking at the results listed in Table 1, it is noteworthy to outline that a complete (≈98%) drug elimination out of the heart tissue has been reached by 20th day after a single intravenous injection of therapeutic dose (0.1 DL_{50}, 80–85 mg/kg body weight) in rats. A systemic clearance level, however, is far lower (blood cells 10 days retention, Fig. 17; blood plasma 1 day retention, Fig. 14). At the same time, all parenchymatic organs tested (skeletal muscle, kidney, lung, liver, brain) do not retain the drug and/or its metabolites for longer than 16–18 h (Fig. 12; Table 1).

In myocardium, the separate and targeted PMC16 delivery of magnetic (^{25}Mg) and non-magnetic (^{26}Mg) isotopes provides an extremely high level of ATP production once the magnetic isotope has been applied (Figs. 8 and 9). The difference in ^{25}Mg/^{26}Mg activation effect values is estimated as high as 2.2–2.5-fold. This might be elevated even up to 3.5 when the PMC16 in vivo does increase from 20 to 30–35 mg/kg (i.v.).

The PMC16 high-safety expectations correlate nicely with what we found investigating the drug related iron metabolic turnover (Fig. 15). A single [^{59}Fe]PMC16 injection leads to a consequent time-dependent appearance of the gamma-emitting label in such natural metabolism participants as heme (hemoglobin, myoglobin), hepatic tissue ferritin and blood plasma transferrin. A kinetics of the latter processes fits the general level of the PMC16 hepatic excretion specified above (Table 1). All together, this is a factor favorable to the metabolically useful and, therefore, potentially safe biotransformation of the PMC16 porphyrin domain [45].

As seen from Table 1, renal excretion of PMC16 is equal to 28.5% and hepatic excretion equals to 16.0%. The nanodrug tested has no affinity to the plasma proteins (1.2% binding) whereas it provides a rather high level of the blood cells uptake: 28.6% for lymphocytes and 8.0% for erythrocytes. The hepatic metabolism leads to the formation of biologically safe urine-eliminated fullerene derivatives such as alanyl-depleted PMC16 (54.6% of total metabolites amount), deacetylated PMC16 derivatives (27.0%) and cyclohexyl-C_{60}-fullerene (16.2%). In a 24 h-collected urine, about 3% of pure C_{60}-fullerene has also been found (Fig. 16).

Both water-soluble and water-insoluble metabolites (products of the PMC16 metabolic degradation) were detected and identified in urine (see Section 2) due to their extraction by CS_2/acetone out of the lyophilized urine dry matter (24 h-collected urine) [1,12,14]. Drug hydrolytic degradation observed is one of the common xenobiotic metabolism pathways, in addition to alkylation, oxidation and conjugation [26,27,31]. Hepatic hydrolases and transferases are major enzyme families involved [31,35,36].

In a classical Ruggher's rat blood cells monitoring experiment, the PMC16 uptake has been tested in lymphocytes and erythrocytes separately using the [^{59}Fe]PMC16 preparations with not less than 470–520 Ci/mmol specific activity (30 mg/kg or 10–12 Ci/kg, i.v. single injection with a following 280 h long-term gradual in-cell label estimations). The lymphocytic drug retention time does not exceed the 280 h limit getting to a highest drug content level within 80–120 h time interval. In erythrocytes, the total retention time is about 120 h with the 1–40 h covered drug cell concentration peak (Fig. 17).

So unlike blood plasma proteins, blood cells may retain an unmetabolized drug for not longer than 120 h (erythrocytes) and nearly 200 h (lymphocytes). A total drug blood cells uptake, however, is rather low being estimated as 7.5–8.5% of the whole dose injected (Table 1, Figs. 15 and 17). According to Refs. [2,36–38], the saturation of lymphocyte membranes with fullerene derivatives of many kinds would hardly cause any immunological

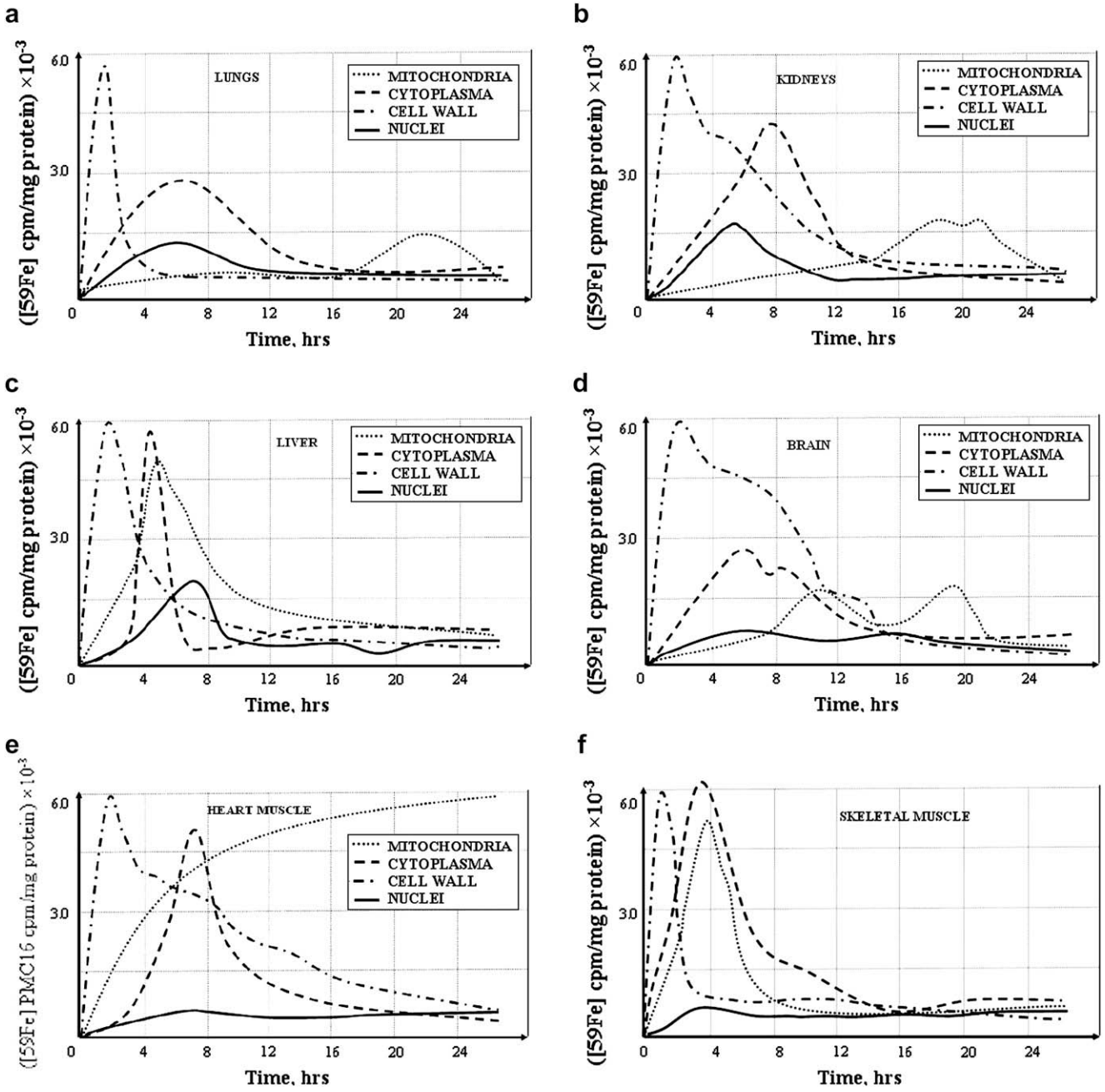

Fig. 12. The cell compartment retaining distribution of [^{59}Fe]PMC16 caused by a single i.v. administration in rats (30 mg/kg, 470–520 Ci/kg). A: lungs; B: kidneys; C; liver; D: brain; E: heart muscle; F: skeletal muscle.

dysfunctions. Under a normal metabolic condition, no $^{25}Mg^{2+}$ release is expected in [$^{25}Mg^{2+}$]PMC16 administration. Unless the hypoxia determined acidosis "commands" so, no paramagnetic magnesium intervention would affect the ATP synthesis in lymphocytes. This should be treated as an additional proof in favor of the drug safety.

The data presented are in a good accordance with a pre-calculated pattern [2] estimating the efficiency of our scheme of the myocardium reception dependent drug targeted delivery (Figs. 10 and 13) as equal to about 75%. In other words, nearly 75% of all single injection inserted drug molecules are retained inside the receptor-rich heart muscle whereas the rest of the drug pool is in fact distributed between the hepatic metabolism reservoir (16–17%) and the limited blood cells uptake (7–9%).

So the PMC16 hepatic turnover relates predominantly to the porphyrin domain decomposition leading to the formation of the biologically neutral heme precursors (Figs. 15 and 16). Along with a high rate of the renal drug elimination (Table 1), this allows to consider the PMC16 particles safe enough for a low dose chronic administration.

Since the PMC16 looks to be a promising tool for myocardium protection in some drug-induced hypoxia cases (Figs. 5–7), we were unable to escape from being involved into certain pharmacokinetic tests on experimental hypoxia models. The most valuable part of this segment of our work is shown in Fig. 18. No matter what particular model of hypoxia tested, just very slight, moderate, changes in the PMC16 pharmacokinetics were observed. Thus, hypoxia promotes nearly 8–8.5% increase of $T_{1/2}$ elevating it from

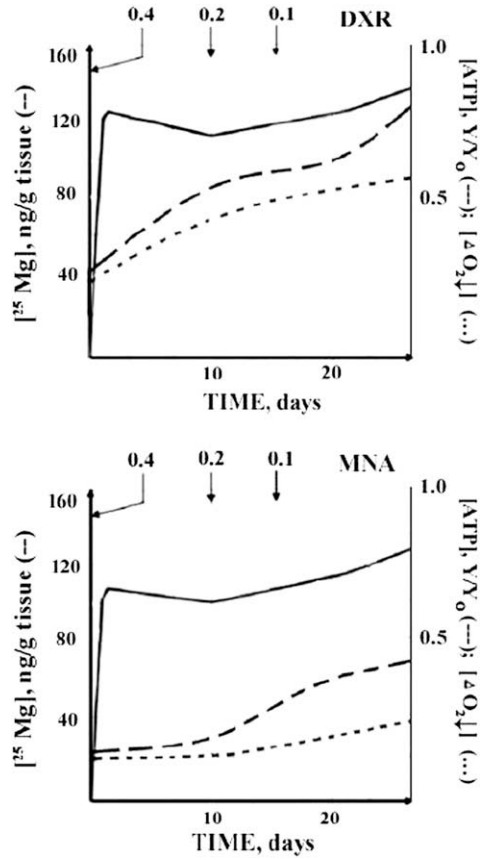

Fig. 13. The rat myocardium tissue respiration affected by DXR and MNA in a course of [$^{25}Mg^{2+}$]PMC16 administration (0.4 → 0.2 → 0.1 mg/kg i.v.). DXR, 80 mg/kg/24 h, i.v.; MNA, 20 mg/kg/24 h, i.v.

9.0 h to about 9.7–9.8 h. Besides, both renal and hepatic excretion processes got slower and changed from 28.5% to 22.0% and from 16.0% to 12.2%, respectively. There is no any serious hypoxia-related impact on the drug blood cells uptake at all. As for the formation of particular drug metabolites, they themselves as well as their ratios are absolutely the same compared to the intact, normal, tissue metabolism conditions (Table 1, Figs. 15, 16, and 18).

In a separate series of experiments, such specific drug metabolism parameters as the PMC16 ^{59}Fe loss degree and the PMC16 hepatic deacetylation degree were investigated for correlation with the hepatic oxygen consumption level (Fig. 18). In the inhalation oxygen-depleted hypoxia, the deep porphyrin domain decomposition does not practically occur while the drug deacetylation rate had decreased by approx. 25% compared to the intact hepatic

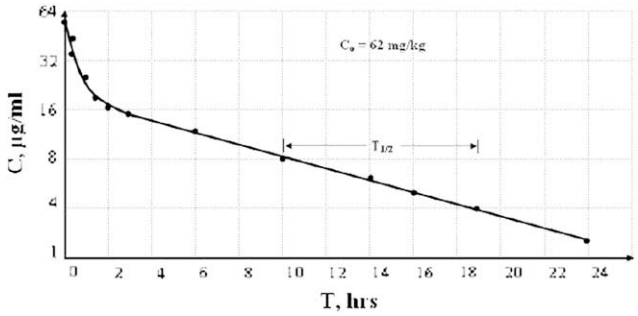

Fig. 14. Systemic clearance: a multiexponential two-compartment dynamics of the blood plasma [Mg]PMC16 concentration after a single 20 mg/kg i.v. injection in rats.

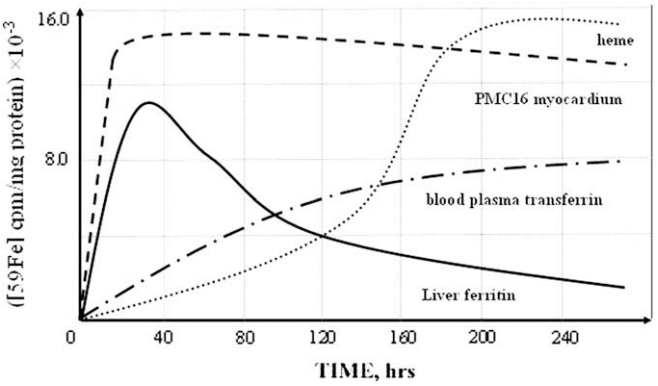

Fig. 15. The PMC16-related ^{59}Fe turnover in rat (20 mg/kg, 380–420 Ci/kg [^{59}Fe]PMC16, single i.v. injection).

metabolism. In contrary, the MNA-promoted hypoxia leads to reversed phenomenon which is up to 80% deacetylation slowing down with roughly 60–65% suppression of the porphyrin domain decay rate.

So the hypoxia conditions, whatever mechanism is behind it, make the drug more resistant to the hepatic metabolic attack. This is considered as an essential and positive supplement to "pharmacological image" of the drug tested [46,47].

The data presented fit our standpoint on essential pharmacological perspectives of the PMC16 as a nanomedicinal agent even though extensive further studies are required. For time-being, however, these results meet some major expectations usual for the new drug pre-clinical trial anyway.

Thus, the most promising key point about the drug tested is that it may provide a truly remarkable (approx. 70%) sliding down of the heart tissue oxygen consumption requirement (Figs. 8 and 9). The drug clearly promotes an essential fall of the myocardium sensitivity to oxygen hunger whatever cause beyond. What seems clinically valid about it, the drug allows to avoid or minimize all pathological consequences of hypoxia in the heart like the contractile strength weakness or arrhythmic disorders.

As per the toxicity/safety patterns of PMC16, they make it suitable for further pre-clinical study since its hepatic metabolism turnover leads to the conversion of the drug porphyrin domain into a normal heme molecule while the cyclohexyl fullerene residues are to be totally eliminated by kidneys with no sign of acute toxicity of these C_{60}-derivatives. The data presented in this paper give a firm reason to expect that the new nanodrug family proposed would attract attention of medical and veterinary professionals engaged in the fields of sports and military medicine, veterinary pharmacology, extreme physiology studies and all clinical disciplines that deal with pre-ischaemic and ischaemic heart function disorders as long as a pathogenesis of the latter is about to deplete a myocardium oxygen availability/consumption.

There are actually the very few precedent studies close enough to the work we have done [20,48–52]. Thus, some bacteriostatic agents based on the oxypiperidine-modified fullerenes are found to be hepatotoxic in rats and rabbits although there is no proof for the high drug systemic clearance rate found for any tissue-specific accumulation [20,52]. Amino acid modifications of fullerene-C_{60}, on a contrary, are found safe due to their fast and complete hepatic metabolism followed by a total renal excretion in rats [49,50]. The latter agents show no trends for the long-term tissue-selective retaining of any sort in either acute [49,53] or chronic [53] experiments in mice and rats. Purine nucleosides were used to functionalize the fullerene-C_{60} surface with following tests of the resulting products for their anticancer activity in hepatoma possessing rats [50]. No asymmetrical distribution of these agents

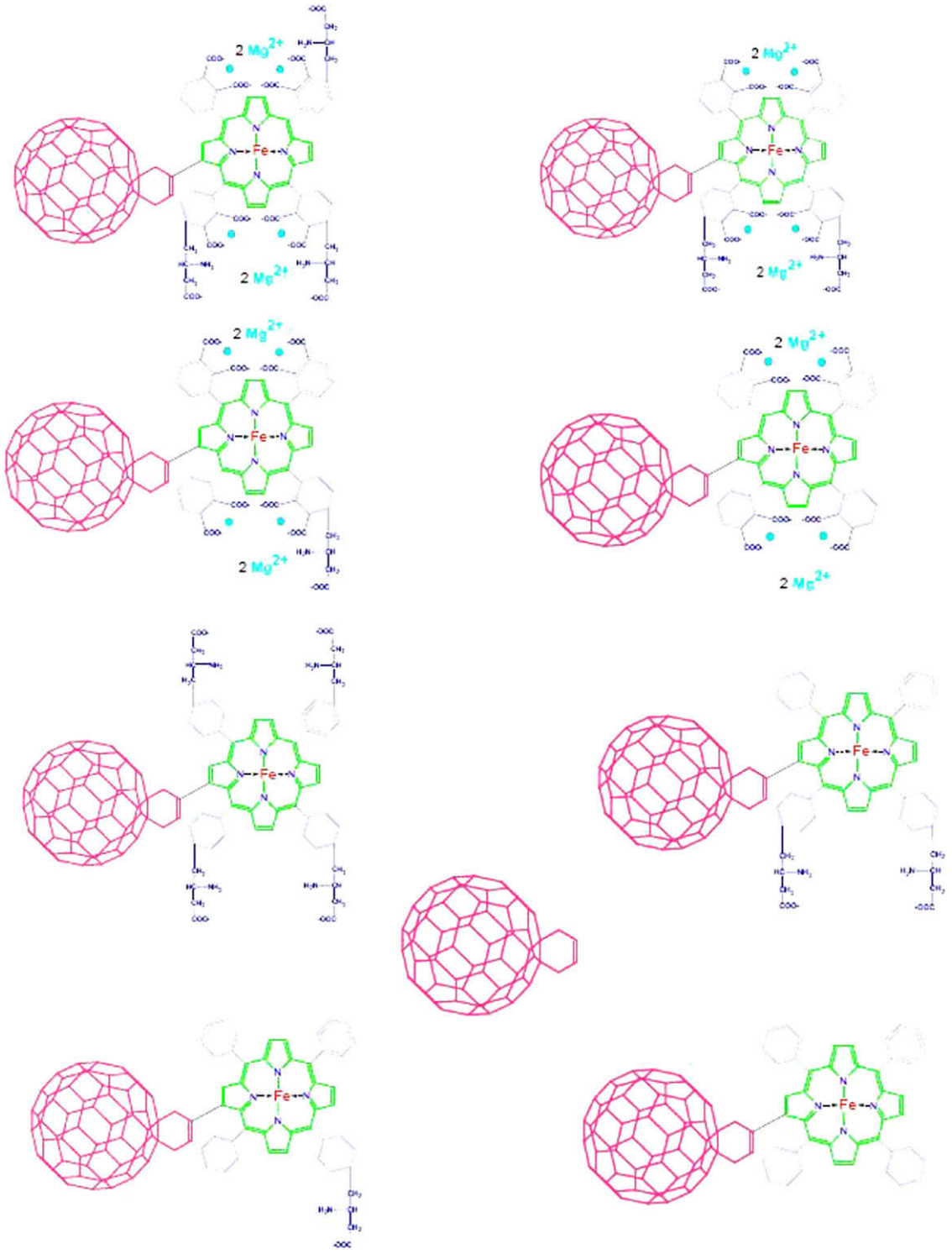

Fig. 16. PMC16 metabolites resulting in the drug hepatic turnover.

was found except for their marked tendency of hepatocyte uptake [50,53]. Riboflavin–fullerene and pyrrolidine–fullerene adducts are to be accumulated predominantly in the secretory epithelial cells while the rest of the mammalian cell/tissue pool remains a non-hosting compartment for these chemicals [20,48,51,53].

It should be mentioned that some water-soluble C_{60}-fullerene derivatives are found to be capable of selective accumulation inside mammalian mitochondria [54] which corresponds roughly to our above listed data on PMC16 pharmacokinetics (Figs. 5, 11, and 12E).

However, no porphyrin adducts of fullerene-C_{60} were ever studied for pharmacological properties prior to our work.

As per the PMC16 zero affinity to the blood plasma proteins, there are some data on the unique (extra low) affinity of the polyalkylated heterocyclic adducts of fullerene-C_{60} to acidic proteins. Even though this might look unusual, there is a firm chemical background beyond that [20,21,36,38]. In short, a hydrophobic fullerene and a heavily carboxylated (negatively charged) porphyrin domain of the drug are hardly compatible with most

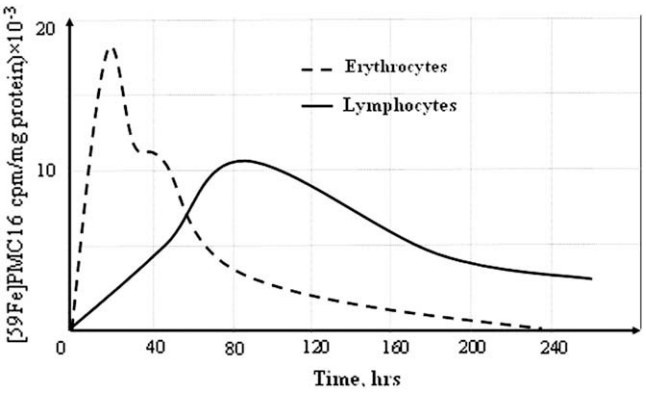

Fig. 17. The PMC16 blood cells uptake in rats. Single i.v. injection, 30 mg/kg [^{59}Fe]PMC16, 470–520 Ci/kg.

abundant functional radicals of the major blood plasma proteins (albumin and globulin sub-populations first).

So we are treating a lack of the marked drug–protein affinity (blood plasma proteins) as a quite expected result except the obvious case of a high-affinity recognition of the drug particle by the cardiac-specific membrane receptor(s) known for their porphyrin-binding properties [2,14,16,44–47], Figs. 5 and 10–12.

Replying some other drug toxicology concerns, the following two statements are to be made.

First, the mass spectrometrically identified PMC16 metabolites (eliminated through the renal excretion) are found to be the low toxic urine-eliminating compounds in numerous studies conducted in the past 3–4 years [20,36,44,46]. Thus, a monograph [20] alone contains a summarizing analysis of over 1000 individual fullerene-C_{60} derivatives' acute toxicity and biological activity patterns. Indeed, some of them are not safe for chronic use although a very few of them have a truly high acute toxicity level. There is a regularity to be mentioned here: once the cyclohexyl-interfaced porphyrin adducts of fullerene-C_{60} tested, the more functionalized the product is, the less acute toxicity level it shows, and vice versa [20,44,46]. An acute toxicity of a pure non-functionalized cyclohexyl-C_{60}, for example, is equal to $DL_{50} = 577–840$ mg/kg, i.v., for different lab mammals (rats, mice, guinea pigs, hamsters), which is far less toxic than such a common pharmaceutical as benzodiazepine anxiolytics or penicillin group antibiotics [20,30].

Secondly, numerous data specified in available literature show the polyphenyl-, oligophenyl-, sorbitol-, heterocyclic-, porphyrin-, and amino acid-modified negatively charged fullerenes as perfectly non-allergenic products with no tendency to intervene in reactions of immunological response of any sort [20,30,34–37]. This is what we consider an additional argument supporting the statement on a good safety potential of the nanoparticles tested.

Concerning the blood–brain barrier (BBB) permeability of the drug, the following should be stressed out. According to our rough estimations, about 0.6% of the [^{59}Fe] label is to appear in the brain tissue homogenate fractions including some cell compartments isolated (Table 1; Fig. 12D) when the [^{59}Fe]PMC16 species were i. v. administered to rat. But unlike in myocardium, the 0.55–0.60% drug content did not allow to find out a non-destructed (non-metabolized, intact) nanoparticle in biological membranes of the brain using a direct tracing/detection techniques (AFM, SANS, HPLC(CG)–FAB/MS, MALDI, FI/FD–MS – see Section 2). So the question about the BBB permeability to PMC16, as a matter of fact, is still to be answered in forthcoming studies.

As seen from the numerous data [30,36,42,44], a vast majority of the fullerene adducts ever tested are unable to penetrate the BBB in mammals. At the same time, some porphyrin-modified derivatives of C_{60} are found to be the BBB-crossing agents although with a very low permeability degree estimated (0.05–0.08% of the i.v. injected intact agent [14]).

In all of these and some other related studies, however, the direct monitoring of the intact drug molecule in a cell (for example, the FAB-chromato-mass spec technique) was not employed so the data quoted are not totally reliable. Therefore, once again, the drug

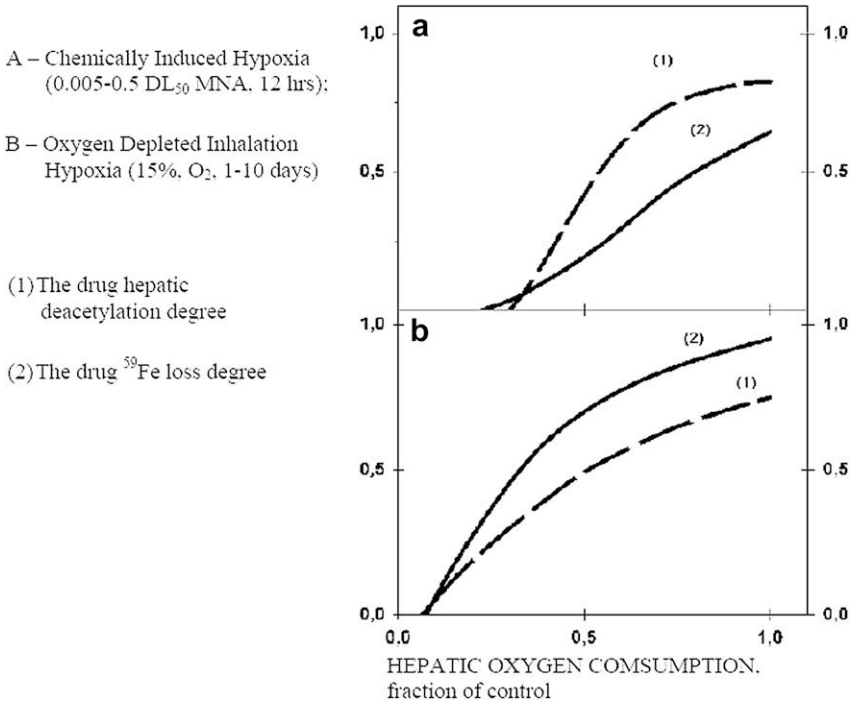

Fig. 18. The hypoxia-affected PMC16 metabolic decay in rat. A: chemically induced hypoxia (0.005–0.5 DL_{50} MNA, 12 h); B: oxygen-depleted inhalation hypoxia (15%, O_2, 1–10 days). (1) The drug hepatic deacetylation degree. (2) The drug ^{59}Fe loss degree.

BBB permeability problem is far from being solved due to the above-specified technological limitations.

The present work is simply focused on the [$^{25}Mg^{2+}$]PMC16 biological activity in the heart.

Regardless of its high affinity to myocardium-specific receptors [55], a pure intact heme is found of being totally non-suitable for Mg^{2+} transportation to the heart due to the following circumstances:

(a) it has no cationite properties, and
(b) it is clearly a subject for fast decompositive biotransformation in vivo (Fig. 15).

Instead, a C_{60}-fullerene nucleus protects the Mg^{2+}-exchanging porphyrin domain from outside enzymatic attack (Figs. 15 and 18) as long as a heavily carboxylated porphyrin K derivative is engaged in the drug structure (Fig. 1).

Hence, the specific peculiarities of PMC16 structure as a combination of porphyrin and fullerene domains provide an advantage of a simultaneous possession of amphiphilic/membranotropic, cation exchanging and low toxic properties associated with a relatively low rate of metabolic decomposition.

As the heart muscle specific PMC16 receptor hypothesized due to a long-term retention of the drug in mitochondria (Figs. 11 and 12E), this receptor was indeed isolated in our parallel study [55]. It turns out that this is a hydrophobic tryptophan-rich 17.6 kDa monomer protein located in an external membrane of the myocardiocyte mitochondria; this protein has a high-affinity to porphyrin ligands of many sorts including PMC16 [55,56].

The last but not the least, the paper presented a first report ever on the medicinal potential of the magnetic isotope effect, a fundamental phenomenon of nuclear chemistry/physics which is still merely unknown to medical professionals [9,11]. So the most important message is a need for a special attention to the [$^{25}Mg^{2+}$]-induced paramagnetic effect in myocardium once this isotope is targeted towards a hypoxia suffering heart muscle due to a novel medicinal smart nanocarrier.

The PMC16 itself is nothing but a carrier for paramagnetic isotope of magnesium. Being not perfect yet, this nanoparticle bears some certainly useful properties. This specific agent is already suitable for laboratory applications as a research tool.

Whatever future the PMC16 would face in practical (preventive or clinical) medicine, the porphyrin adducts of fullerene-C_{60}, as seen from our data presented, deserve to be treated as a new family of pharmacologically promising nanodrugs with respect to the bivalent paramagnetics transportation and their tissue-specific targeted delivery.

4. Conclusions

1. PMC16 is a low toxic membranotropic nanoparticle suitable for the heart muscle targeted delivery of $^{25}Mg^{2+}$ cations needed for the overactivation of ATP synthesis pre-suppressed in the hypoxia damaged myocardium cells.
2. Due to the PMC16-specific receptor location presumably in the myocardiocyte mitochondrial membranes, a selective targeted delivery of the drug might be managed simply by a long-term multiple administration of its low doses. This course provides a marked prophylactic and therapeutic effect in medicinal (chemical-induced) hypoxic cardiotoxicity cases (DXR, MNA).
3. The PMC16 pharmacokinetics shows a myocardium-specific drug retaining beneficial for the reception dependent targeted delivery of [^{25}Mg]PMC16 nanoparticles towards a hypoxia damaged heart muscle.
4. Hypoxia itself slightly increases the nanodrug metabolic stability in vivo.
5. The PMC16 metabolic turnover relates predominantly to the porphyrin domain decomposition leading to the formation of the biologically neutral heme precursors. Along with a high enough rate of the renal drug elimination, this allows to consider the nanodrug safe for a low dose chronic use.

Acknowledgements

This work was supported by the TCO-TUMS NanoBioMedicine Committee and, partly, by the Russian Fundamental Research Support Foundation (Moscow, Russia). The PMC16 synthesis and the nanoparticles $^{25}Mg^{2+}$ loading were performed owing to a technical assistance provided by the Division of Analytical Chemistry, La Sapienza University, Rome, Italy (Prof. L. Campanella) and by the Division of Organic Chemistry, M.V. Lomonosov Moscow State University, Moscow, Russia (Prof. M.A. Yurovskaya). Special thanks to Dr. M.N. Osmolov, the International Nuclear Research Institute at Dubna, Russia, for his exceptional help in getting and analyzing the nanoparticles SANS images. Dr. A. Gupta, Bangalore Center for Cell Biology, India, is to be thanked for his kind help in English style correction.

References

[1] S. Sarkar, S.M. Rezayat, A.L. Buchachenko, D.A. Kuznetsov, M.A. Orlova, M.A. Yurovskaya, I.V. Trushkov, New water soluble porphylleren compounds, European Union Patent No. 07009882.7/EP07009882, Reg.: Munich, Germany, 2007.
[2] S. Sarkar, S.M. Rezayat, A.L. Buchachenko, D.A. Kuznetsov, M.A. Orlova, M.A. Yurovskaya, I.V. Trushkov, Use of a magnesium isotope for treating hypoxia and a medicament comprising the same, European Union Patent No. 07009881.9/EP07009881, Reg.: Munich, Germany, 2007.
[3] K.B. Wallace, A.A. Starkov, Mitochondrial targets of drug toxicity, Annu. Rev. Pharmacol. Toxicol. 40 (2000) 353–388.
[4] A.K. Souid, K.A. Tacka, K.A. Galvan, H.S. Penefsky, Immediate effects of anticancer drugs on mitochondrial oxygen consumption, Biochem. Pharmacol. 66 (2003) 977–987.
[5] K.B. Wallace, Doxorubicin-induced cardiac mitochondriopathy, Pharmacol. Toxicol. 93 (2003) 105–115.
[6] B. Alberts, A. Johnson, J. Lewis, M. Raff, K. Roberts, P. Walter, Molecular Biology of the Cell, Garland Science Publ., NY, 2002.
[7] T. Waugh, H. Telashima, Mitochondria, Research Triangle Publ., Raleigh, Durham, NC, 2004.
[8] A.L. Buchachenko, D.A. Kuznetsov, S.E. Arkhanglesky, M.A. Orlova, A.A. Markarian, Spin biochemistry: magnetic ^{24}Mg–^{25}Mg–^{26}Mg isotope effect in mitochondrial ADP phosphorylation, Cell Biochem. Biophys. 43 (2005) 243–252.
[9] A.L. Buchachenko, D.A. Kuznetsov, S.E. Arkhangelsky, M.A. Orlova, A.A. Markarian, Spin biochemistry: intramitochondrial nucleotide phosphorylation is a magnesium nuclear spin controlled process, Mitochondrion 5 (2005) 67–70.
[10] A.L. Buchachenko, D.A. Kuznetsov, M.A. Orlova, A.A. Markarian, Magnetic isotope effect of magnesium in phosphoglycerate kinase phosphorylation, Proc. Natl. Acad. Sci. USA 102 (2005) 10793–10797.
[11] A.L. Buchachenko, D.A. Kuznetsov, N.N. Breslavskaya, M.A. Orlova, Magnesium isotope effects in enzymatic phosphorylation, J. Phys. Chem., Ser. B 112 (2008) 2548–2556.
[12] K. Kano, Molecular complexes of water-soluble porphyrins, J. Porphyrin Phthalocyanines 8 (2004) 148–155.
[13] R. Hudson, C. Mallroy, S. Darnell, K.M. Smith, Porphyrin conjugates in photoimmunotherapy, Br. J. Cancer 93 (2006) 1442–1450.
[14] R. Pawar, A. Avramoff, A.J. Domb, Nanoparticles for crossing biological membranes, in: C.S.S.R. Kumar (Ed.), Biological and Pharmacological Nanomaterials, Wiley-VCH, Weinheim-Baton Rouge, LA, 2007, pp. 349–393.
[15] D.D. Tyler, J. Gonze, The preparation of heart mitochondria from laboratory animals, Methods Enzymol. 10 (1967) 75–122.
[16] M. Gergely, I. Lakatos, Molecular and Cellular Cardiology, Alba Regia, Budapest, Szeged, 1999.
[17] R. Mahatoo, Biological membranes and barriers, in: I. Telashima, J.A. Waugh (Eds.), Biomaterials for Delivery and Targeting of Proteins and Nucleic Acids, CRC Press, NY, 2005, pp. 241–260.
[18] M.M. Bradford, An improved colorimetric technique for protein measurement, Anal. Biochem. 72 (1976) 348–354.
[19] A.P. Gladyshev, R.R. Asmolov, G.V. Trepova, S.K. Larionov, D.T. Sumarokov, Autoradiography of the ^{59}Fe-labeled organelle supplemented with an electron microscopic track study, Bull. Exp. Biol. Med. 58 (1997) 668–674.

[20] L.B. Piotrovsky, O.I. Kiselyov, Fullerenes in Biology: On the Way Towards Nanomedicine, Rostok Publ., St. Petersburg, 2006, (in Russian).
[21] The Nanofinder-S16E: Laser Confocal Microscopy–Raman Spectroscopy Unit. Technical Manual, Nanofinder Co. Publ., Minsk, Grodno (Byelorussia), 2006.
[22] D.A. Kuznetsov, A.V. Govorkov, N.V. Zavijalov, T.M. Silbileva, V. Richter, J.A. Drawczek, Fast estimation of ATP/ADP ratio as a special step in pharmacological and toxicological studies using the cell-free translation system, J. Biochem. Biophys. Methods 13 (1986) 53–56.
[23] L.W. Lo, C.J. Koch, D.F. Wilson, Calibration of oxygen-dependent quenching of the phosphorescence of Pd-*meso*-tetra-(4-carboxyphenyl)porphine: a phosphor with general application for measuring oxygen concentration in biological systems, Anal. Biochem. 236 (1996) 153–160.
[24] S.A. Vinogradov, D.F. Wilson, Metallotetrabenzoporphyrins. New phosphorescent probes for oxygen measurements, J. Chem. Soc., Perkin Trans. 2 (1995) 103–111.
[25] Radioimmunoassays and Related Analytical Techniques. Technical manual by Bio-Rad, Bio-Rad Press, Durham, St. Petersburg, 2006.
[26] H. Bielka, K. Lottmeyer, K. Roetzsch, O. Schumm, D. Wietzel, M. Rauch, The human blood cells biomass in a drug metabolites uptake screening, Clin. Exp. Pathol. 16 (1996) 444–458.
[27] L.Z. Benet, R.L. Galeazzi, Determination of the steady-state volume drug distribution, J. Pharmacol. Sci. 68 (1979) 1071–1074.
[28] D.J. Morgan, R.A. Smallwood, Clinical significance of pharmacokinetic models of hepatic elimination, Clin. Pharmacokinet. 18 (1990) 61–76.
[29] D.J. Birkett, Pharmacokinetics Made Easy, McGraw Hill Publ., Sydney, Melbourne, 1998.
[30] G. Andrievsky, V. Klochkov, L. Derevyanenko, Is C_{60}-fullerene molecule toxic? Full. Nanotub. Carb. Nanostruct. 13 (2005) 363–376.
[31] M.E. Milanesio, M.G. Alvarez, V. Rivarola, J.J. Silber, E.N. Durantini, Porphyrin–fullerene C_{60} dyads with high ability to form photo-induced charge-separated state as novel sensitizers for photodynamic therapy, Photochem. Photobiol. 81 (2005) 891–897.
[32] Y.L. Lin, H.Y. Lei, C.K. Chou, H.S. Liu, Light-independent inactivation of dengue-2 virus by carboxyfullerene C3 isomer, Virology 275 (2000) 258–262.
[33] T. Mashino, K. Okuda, T. Hirota, M. Hirobe, T. Nagano, M. Mochizuki, Inhibition of *E. coli* grow by fullerene derivatives and inhibition mechanism, Bioorg. Med. Chem. Lett. 9 (1999) 2959–2962.
[34] M. Suarez, Y. Verdecia, B. Illescas, R. Martines-Alvarez, A. Alvarez, E. Ochoa, C. Seoane, N. Kayali, N. Martin, Synthesis and study of novel fulleropyrrolidines bearing biologically active 1,4-dihydropyridines, Tetrahedron 59 (2003) 9179–9186.
[35] D. Pantarotto, N. Tagmatarchis, A. Bianco, M. Prato, Synthesis and biological properties of fullerene-containing amino acids and peptides, Minirev. Med. Chem. 4 (2004) 805–814.
[36] Y. Tabata, Y. Ikada, Biological functions of fullerenes, Pure Appl. Chem. 71 (1999) 2047–2053.
[37] T. Baierl, A. Siedel, The in vitro effects of fullerene black on immunofunctions of macrophages, Fullerene Sci. Technol. 4 (1996) 1073–1085.
[38] M. Mellul, Cosmetic make-up composition containing a fullerene or mixture of fullerenes, US Patent No. 561202, 1997.
[39] J.E. Leone, P.V. Narayanan, Catheter system having fullerenes and method, US Patent No. 6468244, 2002.
[40] L. Schmitt, M. Ludwig, H.E. Gaub, R. Tampe, A metal-chelating microscopy tip as a new toolbox for single-molecule experiments by atomic force microscopy, Biophys. J. 78 (2000) 3275–3285.
[41] D. Fotiadis, S. Scheuring, S.A. Müller, A. Engel, D.J. Müller, Imaging and manipulation of biological structures with the AFM, Micron 33 (2002) 385–397.
[42] M.N.V.R. Kumar, Nano and microparticles as controlled drug delivery devices, Journal of Pharmacy and Pharmaceutical Science 3 (2) (2000) 234–258.
[43] Q.A. Pankhurst, J. Connolly, S.K. Jones, J. Dobson, Application of magnetic nanoparticles in biomedicine, J. Appl. Phys. Series D. 36 (2003) R167–R181.
[44] T. Kubik, K. Bogunia, M. Sugisaka, Nanotechnology on duty in medicinal applications, Curr. Pharm. Biotechnol. 6 (2005) 17–33.
[45] S.C. Gad, Drug Safety Evaluation, John Wiley & Sons, Inc., New York, Boston, Toronto, 2002.
[46] F.H. Hoft, I.B. Hohlfeld, O.V. Salata, Nanoparticles: known and unknown risks, J. Nanobiotechnol. 2 (2004) 12–24.
[47] R. Hong, N.O. Fisher, A. Verma, C.M. Goodman, T. Emrick, V.M. Rotello, Control of protein structure and function through surface recognition by scaffolds, J. Am. Chem. Soc. 126 (2004) 739–743.
[48] P. Rajagopalan, F. Wudl, R.F. Schinazi, F.D. Boudiont, Pharmacokinetics of a water-soluble fullerene in rats, Antimicrob. Agents Chemother. 40 (1996) 2262–2265.
[49] D.F. Emerich, C.G. Thanos, Nanotechnology and medicine, Exp. Opin. Biol. Ther. 3 (2003) 655–667.
[50] O.V. Salata, Application of nanoparticles in biology and medicine, J. Nanotechnol. 2 (2004) 261–268.
[51] S.M. Moghimi, A.C. Hunter, J.C. Murray, Nanomedicine: current status and future prospects, FASEB J. 19 (2005) 311–330.
[52] A. Magrez, S.V. Kasas, V. Salicio, N. Pasquier, J.W. Seo, M. Celio, S. Catsicas, B. Schwaller, L. Forro, Cellular toxicity of carbon-based nanomaterials, Nano Lett. 6 (2006) 1261–1268.
[53] N. Logham, S.M. Pratt, J.A. Crowdell, A. Rodriguez, T. Drumm, P. Wladcziewski, Aromatic and Heterocyclic Derivatives of Fullerene-C60 in the Biological Compartments Distribution Study. Pharmacokinetics and Pharmacodynamics Regularities, in: W. Rattenau, H. Gorowitz (Eds.), Perspectives in Xenobiochemistry, Jagellon Academia Press, Krakow, Poznan, 2008, pp. 467–481.
[54] S. Foley, C. Crowley, M. Smaihi, C. Bonfis, B.F. Erlanger, P. Seta, C. Larroque, Cellular localization of a water-soluble fullerene derivative, Biochem. Biophys. Res. Commun. 294 (2002) 116–119.
[55] N. Amirshahi, R.N. Alyautdin, S.M. Rezayat, S. Sarkar, M.A. Orlova, A.P. Orlov, A.A. Poloznikov, D.A. Kuznetsov, The fullerene-interfaced porphyrin ligand in affinity chromatography of membrane proteins, Chromatographia 68 (2008) 437–441.
[56] N. Amirshahi, R.N. Alyautdin, A.P. Orlov, A.A. Poloznikov, D.A. Kuznetsov, Porphyrin binding membrane proteins in rat myocardium, Russ. J. Phys. Chem. 87 (2008) 623–628.